Journal of Water Process Engineering 50 (2022) 103295

Contents lists available at ScienceDirect

Journal of Water Process Engineering

journal homepage: www.elsevier.com/locate/jwpe

A comparative evaluation of reverse osmosis membrane performance when combined with anaerobic or aerobic membrane bioreactors for indirect potable reuse applications

Yu Huang, Paul Jeffrey, Marc Pidou *

Cranfield Water Science Institute, Cranfield University, Cranfield, United Kingdom

ARTICLE INFO

Keywords:
Aerobic
Anaerobic
Fouling, membrane bioreactor
Reverse osmosis
Water reuse

ABSTRACT

The filtration performance and fouling behaviour of reverse osmosis (RO) membranes was investigated for the post-treatment of aerobic (Ae) and anaerobic (An) MBR effluents treating municipal wastewater for potable reuse. Both MBR effluents followed by RO can produce a water quality sufficient for indirect potable water reuse, while fluorescence excitation-emission scan suggests RO can effectively remove disinfection by-products precursors, ensuring the safety for chlorine based reuse water distribution by rejecting the dissolved organic matters in MBR effluents. AnMBR effluent leads to more fouling when compared to the AeMBR effluent with an average membrane fouling resistance of 12.35×10^{13} m^{-1} and 8.97×10^{13} m^{-1}. Elemental analysis and membrane surface imaging results demonstrate that the foulant deposition sequence is organic and colloidal at first, followed by inorganic substances, while TOC and Ca are the most deposited foulants from both effluents. The unremoved ammonia in the AnMBR effluent may partially go through in the RO permeate and exceed the threshold in Singapore's PUB NEWater standard, while experiencing a significantly higher deposition rate of 13.8 % than the nitrate (0.02 %) from the AeMBR effluent. The findings suggest that the combination of AnMBR with RO offers a more sustainable approach than with the AeMBR but nutrients removal, with the potential of recovery, is recommended before the RO membranes to limit the fouling propensity and achieve a permeate of sufficient quality.

1. Introduction

Water reuse has the potential to make a significant contribution to overcoming the challenges of water scarcity and growing demands on fresh water supply [1,2]. There are growing numbers of water reuse schemes providing non-potable supplies for agricultural irrigation and industrial cooling in many countries [3,4]. Furthermore, potable water reuse applications are becoming more widely implemented across the world, including surface and ground water recharge schemes which blend treated effluent with raw water before final abstraction for drinking water production (indirect potable reuse) and directly using treated effluent as a source of drinking water (direct potable reuse) [5,6]. To ensure the quality and safety of the purified wastewater, water quality parameters have to be monitored and controlled including organics, nutrients, pathogens, trace elements including for example disinfection by-products (DBPs) [7–9].

In this context, membrane bioreactor (MBR) technologies offer several advantages over conventional treatment systems, delivering a robust, solids free effluent which is substantially disinfected [10]. The combination of a conventional activated sludge process with membrane filtration also significantly reduces the plant footprint [11]. Typical MBR applications are based on aerobic reactors (AeMBR). Anaerobic membrane bioreactors (AnMBR) operating in an oxygen free environment are an alternative form of MBR which has attracted extensive interest in recent years. In comparison to AeMBR, the biological process of an AnMBR digests the organic compounds in the absence of oxygen which requires no energy demand for aeration, and produces a methane rich biogas which offers the potential to produce energy from the methane, leading to lower energy consumption as well as a further reduced footprint [12,13].

Reverse osmosis (RO) filtration is commonly used for potable reuse applications [14–16]. With a typical pore size between 0.1 and 1.0 nm these membranes allow the rejection of the smallest contaminants and monovalent ions [17]. The combination of RO with AeMBR has been

* Corresponding author.
E-mail address: m.pidou@cranfield.ac.uk (M. Pidou).

https://doi.org/10.1016/j.jwpe.2022.103295
Received 6 September 2022; Received in revised form 14 October 2022; Accepted 31 October 2022
Available online 18 November 2022

shown to deliver a reliable and high quality effluent for potable water reuse [14,18] specifically when strict organic micropollutant threshold values are set [15,19]. Indeed, the combined systems have been shown to remove almost 99.9 % of particles, pathogens, viruses, and organic micro-pollutants (OMPs), as well as the vast majority of nutrients, thus posing no organic and pathogen concerns as the resulting effluent has high bio-stability [20]. These advantages raise the possibility of combining RO with AnMBRs to produce potable reuse quality effluent but with lower overall energy consumption. In this context, Gu et al. have reported a combined AnMBR-RO-IE (ion exchange) system able to produce NEWater-like water [21,22] while recovering energy. However, the effluents from AeMBRs and AnMBRs have different matrices that may impact the RO filtration performance and in particular the fouling mechanism differently. Shin et al. [23] reported that at pH 6, the total ammonia nitrogen rejection efficiency of RO was optimal at 99.8 % and Liu et al. [24] suggested that the presence of N and P at higher levels may lead to severe membrane fouling due to biofilm formation. Available literature comparing the performance of AnMBRs with AeMBRs is focusing on several aspects, as for example, Wang et al. [13] demonstrated that AnMBRs have a better energy efficiency treating municipal wastewater compared to AeMBRs, Zaouri et al. [25] showed that both AeMBR and AnMBR effluents have different organic and nutrient content as well as concentrations of emerging contaminants and heavy metals, and Liu et al. [26] reported a higher removal of most trace organics (TrOCs) by AeMBR while AnMBR effluent has a higher level of TrOCs with nitrogen in their molecular structures. However, no literature has been found which focuses on the comparison of AnMBR and AeMBR effluents for potable reuse applications, and more specifically on how the different matrices produced by the aerobic and anaerobic systems will impact the treatment and operational performance of the reverse osmosis membranes.

Several studies which have looked at potable water reuse through an AeMBR-RO system have focused on the fate of TrOCs [27–29]. Other studies have reported that the organic matter in MBR effluent plays an important role in the evolution of RO fouling [30] and that the incomplete removal of nitrate by the RO membrane poses a potential concern of catalysing DBP formation [31,32]. RO processes can simultaneously remove both organic and inorganic DBP precursors thereby providing an important option for DBP minimization [33]. Studies on AnMBR-RO systems are very few compared to those on AeMBR-RO. Despite this interest in coupling AnMBRs with RO for reuse, several knowledge gaps remain if we are to better understand the feasibility of AnMBR-RO systems for potable water reuse, specifically the impact which the different effluent matrix, when compared to an AeMBR, may have on treatment performance and fouling mechanisms. The fate of DBP precursors through each technology is also unclear. Therefore, a comparative evaluation of reverse osmosis membranes combined with both anaerobic and aerobic MBR treating municipal wastewater for potable reuse applications would provide significant advances in the field.

This paper is then the first direct comparison between an AnMBR and an AeMBR treating real municipal wastewater for potable water reuse when coupled with reverse osmosis membranes and compares the performance of both options against a comprehensive range of water quality parameters and trace elements listed in PUB's NEWater standard for potable reuse. It also specifically examines the impact of various key species on RO fouling from each effluent. The major RO foulants were qualitatively and quantitatively characterized for the AnMBR and AnMBR effluent, respectively.

2. Materials and methods

2.1. Pilot scale anaerobic membrane bioreactor and aerobic membrane bioreactor

AnMBR and AeMBR pilot plants (Fig. 1) were installed in Cranfield University's National Research Facility for Water and Wastewater Treatment and operated stably for 55 weeks. The systems were fed with the raw wastewater from the Cranfield University sewage works after settling in a primary settling tank. The AnMBR was configured as a cylindrical upflow sludge blanket bioreactor (UASB-45 L) and a side stream membrane tank (30 L), seeded with granular sludge obtained from a system treating industrial wastewater from the paper industry (Saica Paper, Manchester, UK). The sludge was acclimatised to the settled wastewater for 21 days until performance stabilised before focused trials started. The settled municipal wastewater was fed by a peristaltic pump (Watson Marlow 620 s, UK). Internal recirculation

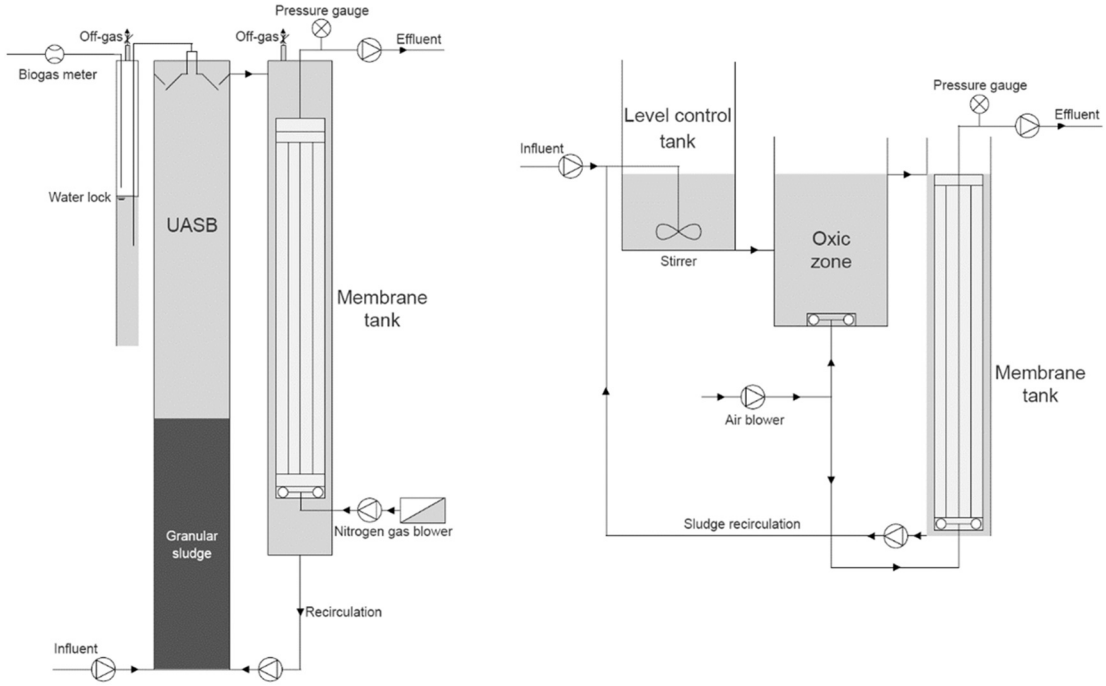

Fig. 1. Process flow diagram for AnMBR and AeMBR

between the membrane tank and the UASB reactor was maintained by a peristaltic pump (Watson Marlow 520 s, UK). The AnMBR was operated under ambient temperature with a 0.9 m/h upflow velocity, 8 h hydraulic retention time (HRT), and infinite sludge retention time (SRT). The AeMBR was configured with a level control tank (10 L), aerobic tank (40 L) and membrane tank (18 L), seeded with activated sludge obtained from the Cotton Valley sewage treatment works (Anglian Water, Milton Keynes, UK). The AeMBR was operated under ambient temperature with 12 h HRT and 7 days SRT. DO in the aerobic tank was controlled to above 1 mg/L and the mixed liquor suspended solids in the membrane tank was controlled between 8000 and 12,000 mg/L. Recirculation was maintained by a peristaltic pump (Watson Marlow 520 s, UK) at the rate of 200 %. For both systems, a PVDF hollow fibre ultra-filtration (UF) membrane with 0.93 m^2 surface area and 0.04 μm nominal pore size (GE ZW-10, USA) was placed in the membrane tank and operating with a flux of 10 LMH. Permeate was produced by suction through a timer controlled peristaltic pump (Watson Marlow 520 s, UK) with 60 min permeation and 30 min relaxation periods. For the AnMBR, nitrogen gas was continuously sparging into the membrane module with a constant specific gas demand of 0.25–1.0 m^3m^{-2} h^{-1}. For the AeMBR, compressed air was continuously sparging into the aerobic tank and membrane module through a fine air bubble diffusor at a rate of 0.93 m^3h^{-1} and a course air diffusor for a specific aeration demand of 0.25–1.0 m^3m^{-2} h^{-1}, respectively. Due to the conservative approach in the operation of the membranes, during the 55 weeks of operation of the two MBRs, no membrane cleaning was required.

2.2. Bench scale reverse osmosis membrane cell

A dead-end bench scale (300 mL) reverse osmosis (RO) membrane cell system (Sterlitech HP4750, USA) was used for the filtration tests with the effluents from both AnMBR and AeMBR. The pressure driven filtration was achieved with a pre-cut 47 mm diameter polyamide-urea-thin film composite hydrophilic flat sheet low fouling reverse osmosis membrane (TriSep X201, USA), recommended for applications such as water recycling, with an active membrane area of 14.6 cm^2. For the tests, a constant 10 Bar pressure was maintained by a regulator (BOC, UK) with bottled oxygen free nitrogen gas (BOC 1066, UK). A constant 400 RPM stirring rate was maintained with a magnetic stirrer (Benchmark 3770, UK) to mix the MBR effluents and limit concentration polarisation at the surface of the membrane. For each test, a 60 mL sample of the AnMBR/AeMBR effluent was sealed into the membrane cell and filtered with a new RO membrane coupon until a recovery of 75 % was achieved. After the filtration, the 45 mL RO permeate and 15 mL RO concentrate samples were analysed. The new RO membrane coupon was first soaked in deionised (DI) water (ELGA, UK) for 12 h prior to the filtration test. Clean water flux tests were carried out with DI water before and after each filtration test to determine the clean water permeability with and without fouling and allow the calculation of the resistance. For the clean water test, the filtration time for 5 mL of DI water was recorded.

Membrane fouling resistance was calculated with the equation according to Darcy's law:

$$R_f = R_t - R_0 = \frac{P}{\mu \bullet J_t} - \frac{P}{\mu \bullet J_0} \quad (1)$$

where, R_f (m^{-1}) = resistance of fouling layer, R_t (m^{-1}) = total resistance at time t, R_0 (m^{-1}) = clean membrane resistance, t (s) = filtration time, J_0 ($m^3{\cdot}m^{-2}{\cdot}s^{-1}$) = clean membrane flux, J_t ($m^3{\cdot}m^{-2}{\cdot}s^{-1}$) = flux at time t, p (Pa) = pressure, μ ($Pa{\cdot}s^{-1}$) = DI water viscosity = 0.01.

Deposited foulants mass was calculated with the equation according to mass balance law:

$$m_{ROD} = C_0 \times 60 - C_{ROP} \times 45 - C_{ROC} \times 15 \quad (2)$$

where, m_{ROS} (μg) = mass of the substance deposited on the RO membrane surface (ROS), C_0 (μg/L) = substance concentration in the RO feed, C_{ROP} (μg/L) = substance concentration in the RO permeate (ROP), and C_{ROC} (μg/L) = substance concentration in the RO concentrate (ROC).

The foulant deposition rate was calculated with the equation adapted from Tang et al. [34,35]:

$$R_D = \frac{m_{ROD}}{m_0} \times 100\% \quad (3)$$

where, R_D (%) = the foulant deposition percentage, and m_0 (μg) = mass of the substance in the RO feed.

2.3. Analytical measurements

Temperature, pH and total dissolved solids (TDS) were measured by an online probe (Endress+Hauser, Switzerland). Total suspended solids (TSS), 5 day biochemical oxygen demand (BOD_5), sludge volume index (SVI) were measured based on the Standard Methods [36]. Chemical oxygen demand (COD), ammonia nitrogen (NH_3−N), nitrite (NO_2-N), nitrate (NO_3-N), phosphate (PO_4-P), and total phosphorus (TP) were analysed with cell tests and a photo spectrometer (Merck Spectroquant, Germany). Total coliform (TC), Faecal coliform (FC) and Escherichia coliform (*E. coli*) were measured by Quanti-Tray (Coliler-18, USA) analysis. Total organic carbon (TOC) and total nitrogen (TN) were measured by a Shimadzu TOC analyser (Shimadzu 3201, Japan). Trace level elements were analysed with an inductively coupled plasma mass spectrometry (ICP-MS) (PerkinElmer NexION 350d, USA). Characterization of the MBRs influents were measured after filtering with 0.45 μm syringe membrane disc filter (Merck Millipore, Germany). Organic composition was evaluated by a fluorescence spectrometer (HORIBA FLuoroMax+, Japan) with a 3D excitation–emission matrices. Scan settings were 200–400 nm excitation and 280–500 nm emission wavelength, 1 nm entrance slit and an integration time of 0.1 s. The 1st and 2nd Rayleigh scatter were masked with 5 nm slit width by FluorEssence software (HORIBA, Japan). The fluorescence intensity maps were masked together by light intensity order to increase the accuracy while minimizing the signal noise and system error. Each map displayed a colour metric bar to quantify the detected peak intensities, where the intensity shifted from low to high within blue-green-yellow-red. Results from Fluorescence spectrometer were plotted as a 2D intensity map and the fluorescence regional integration (FRI) analysis was extracted with a 5 region DOM categories method (aromatic protein (AP): tyrosine-like (APr) excitation/emission (E_x/E_m) = (200–250) nm/(280–330) nm; tryptophan-like (APy) E_x/E_m = (200–250) nm/(330–380) nm; fulvic acid-like (FA) E_x/E_m = (200–260) nm/(380–500) nm; soluble microbial products (SMP) E_x/E_m = (250–280) nm/(310–380) nm; humic acid-like (HA) E_x/E_m = (280–380) nm/(380–500) nm) [37,38] using an R scrip modified from Lapworth and Kinniburgh [39]. The foulant layer accumulated on the RO membrane coupons during the filtration process was characterized by a scanning electron microscope with energy dispersive spectroscopy (SEM-EDS) for imaging (Tescan S8000G, Czech Republic) and EDS (Oxford Instruments Ultim Max detector, UK) analysis with AZtec software (Oxford Instruments, UK). A virgin RO membrane and fouled membranes obtained from each filtration batch (5 AnMBR-RO and 5 AeMBR-RO) were dried under constant room temperature before a 1 cm^2 piece was cut from the centre of the membrane. The cut membrane was then adhered to a carbon tab and coated with 10 nm gold, finally the coated membrane sample was transferred to the SEM-EDS. SEM imaging was done in secondary electron mode for topography, EDS analysis was done for 5 selected areas on each site in SEM images with backscatter mode under low vacuum for atomic number contrast. Raw numerical data was input to JMP 16 pro to obtain a multivariate correlation analysis and statistical analysis.

3. Results and discussion

3.1. MBRs influent and effluents quality

Typical municipal wastewater parameter values were measured for the influent feeding the two MBRs, with a slightly lower strength (BOD_5/COD = 0.38) compared to others reported in the literature on MBR systems (B/C > 0.5) [40–42]. This can be explained by the fact that the majority of the trials were conducted during the COVID pandemic and that the population on the university campus was lower than usual which would have affected some of the characteristics of the raw sewage. There was no organic phosphate detected during the whole period of the experiment and the concentration of total phosphorus (TP) was equal to that for PO_4-P (Table 1).

Similar pH values were measured for the AnMBR (7.6) and AeMBR (7.5) effluents and the temperature was almost the same since both reactors were operated under ambient temperature. Under this pH, ammonia was mostly in the form of ammonium (NH_4^+) under which conditions a lower ammonium removal (97 %–99 %) may be expected during RO filtration [23]. The AnMBR effluent had a slightly higher total dissolved solids (TDS) concentration than for the AeMBR, indicating there was more dissolved content to be sent on to the RO membrane. Due to the UF membrane, total suspended solids (TSS) and coliforms (TC, FC and *E. coli*) were not detected in both effluents. This is in agreement with previous literature which has highlighted that there is no concern with TSS and coliforms under undamaged membrane conditions [43], as well as the evidence for satisfying the NEWater standard's threshold for microbial barrier even before the RO filtration. Additionally, this suggested there should be no particulate fouling and limited biofouling formation on the RO. In terms of organic removal performance, the AeMBR achieved a better removal of COD (95 %), BOD_5 (97 %) and TOC (73 %) compared to the AnMBR with 83 %, 89 % and 27 %, respectively. The unremoved organics may cause organic fouling of the RO membrane and decrease the filtration performance since the adsorption of organic substances onto the membrane surface has been shown to form an organic film contributing to fouling [44]. Phosphate levels of the two effluents were very similar, although the AeMBR effluent had a slightly higher concentration as a result of high SRT and MLSS. Literature has suggested the presence of phosphate can cause inorganic scaling in particular with calcium phosphate, and simultaneously absorbing silica onto the surface hydroxyl functional groups, which also causes silica deposition on the RO membrane surface since phosphate polymers are structurally very similar to those of silica [45]. There was no nitrite (NO_2-N) detected in both effluents. However, other nitrogen species, specifically ammonia nitrogen (NH_3-N) and nitrate (NO_3-N), were found to constitute the largest difference between the AnMBR and AeMBR effluents. There was no nitrate detected in the AnMBR effluent and nearly no removal was found for ammonium. Oppositely, for the AeMBR effluent, there was no ammonium and 17.6 ± 4.4 mg/L of nitrate. This can be explained as a function of the different biological processes happening before the membrane modules. Anaerobic biomass converts organics to methane-rich biogas and also reduces the nitrate and nitrite to ammonia in the absence of oxygen while the aerobic process oxidises the ammonia to nitrite then to nitrate with biological nitrification in the presence of oxygen [12,46]. A minor difference in the TN removal was found between the two MBR effluents, which may be explained by the different organic nitrogen (Or-N) removal during the biological stage, where the AeMBR removed more Or-N in the presence of oxygen compared to the AnMBR. Interestingly, there is no literature on the impact of ammonia and nitrate on RO fouling and this may be a critical insight to understand the fundamental role for AnMBR combined with RO as a post-treatment process for high grade water reuse applications.

Trace element analysis displayed similar results for the AnMBR and AeMBR effluents. There was no meaningful removal of Fe or Cu whereas the low levels of Cd and Pb in the influent streams were below the limit of detection. Levels of B, Na, Mg, Si, K, Ca, Cu, Zn, Sr, and Ba in the

Table 1
Water quality parameters and trace level elements analysis for the influent wastewater, AnMBR and AeMBR effluent during the 55 weeks of operation.

Unit	Influent		AnMBR effluent		AeMBR effluent	
mg/L	Mean	Std	Mean	Std	Mean	Std
pH	7.9	±0.5	7.6	±0.5	7.5	±0.4
°C	14.3	±5.3	13.3	±6.2	13.4	±6.2
TDS	410.4	±64.8	379.2	±72.6	304.5	±77.5
TSS	112.1	±31.1	ND*		ND*	
COD	218.9	±59.4	37.6	±15.5	10.1	±8.5
BOD_5	83.3	±39.7	9.3	±6.5	2.7	±1.7
TOC	24.6	±5.5	17.9	±5.8	6.7	±1.3
NH_3-N	23.7	±5.3	25.0	±7.0	ND*	
NO_3-N	0.9	±1.8	ND*		17.6	±4.4
NO_2-N	0.4	±0.6	ND*		ND*	
Or-N	4.5	±1.6	2.3	±0.5	0.5	±0.2
TN	31.3	±4.5	28.8	±6.5	24.1	±3.5
PO_4-P	3.9	±1.4	4.0	±1.2	4.3	±1.5
Or-P	ND*		ND*		ND*	
µg/L	Mean	Std	Mean	Std	Mean	Std
B	54.17	±20.64	73.00	±9.85	64.39	±11.06
Na	44,766.67	±9016.80	50,780.95	±11,015.06	50,647.62	±9502.61
Mg	5283.33	±383.54	5373.33	±329.14	5472.38	±485.74
Al	ND*		ND*		ND*	
Si	7473.33	±552.47	7028.57	±974.55	6840.00	±309.71
K	13,636.67	±1391.89	13,051.43	±2610.50	12,712.38	±1522.31
Ca	42,733.33	±5845.57	48,657.14	±8576.75	49,190.48	±9831.27
Mn	11.43	±6.26	2.08	±5.90	ND*	
Fe	47.15	±20.91	41.65	±14.93	34.12	±17.34
Cu	62.17	±12.89	59.10	±11.41	61.80	±19.62
Zn	6.43	±13.03	11.45	±13.81	16.04	±11.36
Sr	171.57	±38.55	198.65	±44.63	200.12	±51.74
Cd	0.67	±1.59	ND*		ND*	
Ba	45.83	±3.09	37.90	±2.58	36.26	±4.40
Pb	0.04	±0.10	ND*		ND*	

Note: ND*, Non detectable.

effluents remained similar to the influent. However, trace levels of Mn were found in the AnMBR effluent but not in the AeMBR effluent. This was due to the different SRT applied to the two MBRs. The removal mechanism for heavy metals is mainly by sludge sorption [19,47]. The AnMBR in this study was operated with an infinite SRT but for the AeMBR the sludge was discharged regularly each week, therefore the AnMBR sludge had possibly reached the breakthrough point for its sorption capacity. Among those elements detected in the MBR effluents, Fe, Ca, Mn, Si and Mg are reported to be major inorganic elements of RO Membrane surface deposits [34], causing inorganic scaling of the RO membrane [35]. Additionally, the co-presence of silica and organic matter can cause severe membrane fouling for RO filtering MBR effluent, whereas silica alone did not cause severe fouling [30]. This highlights the need to understand the interactions between silica and specific organic matter such as proteins and soluble microbial products (SMPs). Ultimately, the difference in organic matter and nitrogen species may indicate that higher RO membrane fouling should be expected when coupled with an AnMBR compared to an AeMBR.

3.2. RO performance with AnMBR and AeMBR effluents

3.2.1. Indirect Potable water reuse parameters and trace elements

Identical analytical measurement was conducted for the RO permeates (ROP) obtained from the AnMBR and AeMBR effluents (Table 2). The average pH of the RO permeate from the AnMBR (6.0) and AeMBR (5.8) effluents were slightly lower than the Singapore's PUB NEWater standard requirement (7.0–8.5) [48], which could be stabilised by adding lime [6] or blending with another source of water [20,32]. Significant removal of TDS, COD, NH_3-N (AnMBR), NO_3-N (AeMBR), Or-N, TN, PO_4-P, and TOC were found for both permeates and a complete non detectable BOD_5 was achieved, while the TDS for AnMBR and AeMBR permeates was respectively lower than the threshold in PUB NEWater standard [48]. Indeed, only 88 % ammonia and 87 % nitrate removal were achieved respectively in the AnMBR-ROP and AeMBR-ROP. The incomplete removal of ammonia was reported by Qin et al. [49] as the rejection efficiency of ammonia varies with pH and flux due to the presence of deprotonated non-ionic ammonia. Residual ammonia may pose a concern during chlorine based disinfection processes as the formed chloramine can react with aromatic protein-like (AP) substances which results in *N*-Nitrosodimethylamine (NDMA) formation [50–52]. The ammonia concentration in the AnMBR-ROP (4.0 ± 1.9) exceeded the 1 mg/L limit specified in the NEWater standard [48]. This suggests that the pre-removal of ammonia, or a post-polishing process is required when combining RO with AnMBR for indirect potable reuse purposes. Indeed, literature has widely reported that buffering the feed water to an optimal pH range from 6 to 6.5 can significantly enhance the ammonia rejection up to 99.8 % [23,53,54]. Moreover, the presence of ammonia in the AnMBR effluent can be useful for chloramine production before the RO membrane when a chlorine based fouling control regime is applied [55] since also Huang et al. [56] suggested that chloramination achieved with the sequence of adding ammonia then chlorine generates less DBP than adding chlorine followed by ammonia. In contrast, nitrate removal by RO under neutral pH may be reduced in the presence of sodium and sulphates, which has been shown to reduce the removal percentage down to 50 % [57]. However, the nitrate concentration in the AeMBR-ROP met the 5 mg/L regulation limit [48] but Comerton et al. [31,32] have suggested the residual nitrate may cause a concern in the context of DBP formation.

Excellent removal was observed for Mg, Si, K, Ca, Mn, Fe, Cu, Zn, Sr, and Ba in both permeates and the previously reported traces of Mn and Fe in the AnMBR and AeMBR effluents were removed, while the concentrations of B, Na, Al, Si, Ca, Mn, Fe, Cu, Zn Sr, and Ba in AnMBR-ROP

Table 2
RO performance on treating AnMBR and AeMBR effluent.

Unit	AnMBR-RO effluent			AeMBR-RO effluent			PUB NEWater standard
mg/L	Mean	Std	Removal%	Mean	Std	Removal%	[48]
pH	6.0	±1.9		5.8	±1.8		7.0–8.5
°C	13.3	±6.2		13.4	±6.2		
TDS	37.5	±11.7	93 %	33.3	±10.4	92 %	<150
COD	1.9	±2.5	96 %	1.3	±2.1	90 %	
BOD_5	ND			ND			
TOC	1.8	±1.0	92 %	1.1	±0.4	88 %	
NH_3-N	4.0	±1.9	88 %	ND			<1
NO_3-N	ND			3.0	±1.4	87 %	<5
Or-N	ND			ND			
TN	5.3	±1.8	86 %	4.1	±1.2	87 %	
PO_4-P	0.3	±0.3	95 %	0.3	±0.3	95 %	
µg/L	Mean	Std	Removal%	Mean	Std	Removal%	
B	36.73	±11.28	62 %	45.04	±12.89	48 %	<50
Na	5624.44	±1806.15	92 %	7248.89	±2002.88	89 %	<20,000
Mg	222.98	±149.47	97 %	295.56	±149.96	96 %	
Al	ND			ND			<100
Si	475.33	±158.92	95 %	541.47	±283.47	94 %	<3000
K	1566.89	±469.39	91 %	1814.67	±475.72	89 %	
Ca	2024.00	±1226.37	97 %	2830.22	±2016.54	96 %	<20,000
Mn	ND			ND			<50
Fe	5.38	±1.25	90 %	ND			<40
Cu	4.65	±1.16	94 %	7.09	±62.38	91 %	<50
Zn	1.27	±1.89	92 %	1.38	±1.37	94 %	<100
Sr	5.90	±5.12	98 %	8.77	±5.25	97 %	<100
Cd	ND			ND			
Ba	2.34	±1.27	95 %	3.16	±1.01	93 %	<100
Pb	ND			ND			

Note: ND*, Non detectable.

and AeMBR-ROP satisfied the limit in the NEWater standard [48]. However, the rejection rate of Na was 92 % and 89 % for the AnMBR and AeMBR effluent, respectively, which is lower than the manufacturer's specification (98.5 %). This can be explained by the more complex feed water matrix and operating conditions used during the study as compared with the manufacturer's testing regime which uses ultrapure water with dissolved high purity sodium chloride. Low Boron (B) removal was found in both permeates with 62 % and 48 % removal for the AnMBR-ROP and AeMBR-ROP, respectively. This finding agrees with Tu et al. [58] that the Boron rejection rate increases with increasing pH and operating pressure but decreases when temperature and fouling increase. In this study the less preferable feed water pH and operating pressure led to the low boron removal.

Overall, the combination of RO and AeMBR is able to produce a sufficiently high quality permeate for a potential indirect potable water reuse, with inadequate ammonia removal being a notable weakness of the AnMBR-RO combination. The RO step successfully act as the barrier to offset the insufficient organic and phosphate removal in both MBR effluents, as well as the potential heavy metal concern initially observed in the AnMBR effluent.

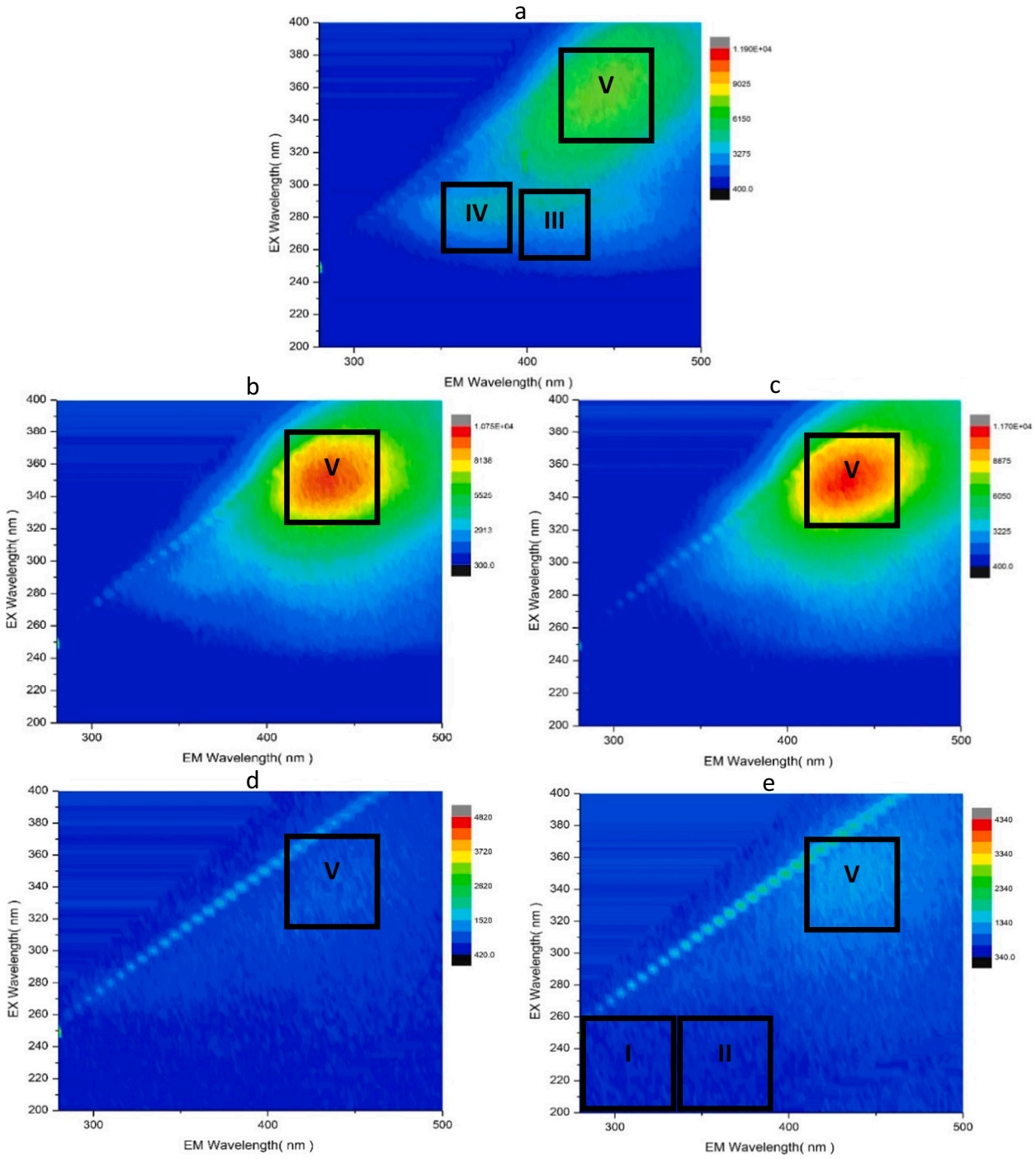

Fig. 2. DOM characterization of (a) influent wastewater, (b) AnMBR and (c) AeMBR effluent, (d) AnMBR-ROP and (e) AeMBR-ROP. Where Zone I: tyrosine-like (APr); Zone II: tryptophan-like (APy); Zone III: fulvic acid-like (FA); Zone IV: soluble microbial products (SMP); Zone V: humic acid-like (HA). (In colour please).

3.2.2. Impact of dissolved organic matter on RO treatment performance

With fluorescence spectroscopy, a wide intense peak present in Zone V indicates the presence of a significant amount of humic acid (HA) (Fig. 2.a), while the peaks in Zones III and IV confirmed the presence of some fulvic acid-like substances (FA) and soluble microbial products (SMP) respectively. The AnMBR (Fig. 2.b) and AeMBR (Fig. 2.c) effluents displayed a similar distribution as both intensity maps have a deep red coloured peak shifted to light green in Zone V, indicating the major substance present is HA. However, the middle left light blue peak in the AnMBR effluent map suggests a higher content of SMP compared to the AeMBR effluent. Both intensity maps of the RO permeates (Fig. 2.d and 2.e) exhibit a large area of blue with noticeable unmasked 2nd order Rayleigh scatter and several light blue peaks in Zone V for HA. However, there was very little indication of aromatic protein (AP) (Zones I and II) present in the AeMBR-ROP effluent and none at all was found in the AnMBR-ROP effluent. This suggests the better removal of DOM will lead to a higher level of membrane fouling during the filtration of the AnMBR effluent [59].

The similar peak distribution for the AnMBR and AeMBR effluent indicates that a similar DOM fouling behaviour should be expected during RO filtration. However, the intensity map only displayed the relative concentration detected in each sample, offering no quantitative comparison. A further Fluorescence Regional Integration analysis (FRI) and mass balance was needed to quantify the concentration of each species. The Ca concentration detected in both MBR effluents in this study exceeded 1 mM, which is reported as the critical value of Ca^{2+} under a neutral pH to bind humic acid molecules together through the bridging effect, and partially neutralize the negative charge on humic acid thereby greatly enhancing the collision efficiency of approaching humic material onto membrane surfaces [60,61]. This finding ultimately highlighted the need for further analysis using SEM-EDS analysis for membrane surface foulant characterization.

As shown in Fig. 3, the use of UF membranes within the MBRs achieved 50 % removal of SMP, the rest of the organic substances presented a low removal particularly for HA as the main removal mechanism is size exclusion. This finding agrees with Liu et al. [62] that although UF has a certain retention for all categories of DOM, the removal efficiency is not high. RO filtration achieved a low removal of AP substances due to the low initial concentration. The RO step removed a further 50 % of SMP and FA after the RO but a sharp reduction of HA was noted in both MBR permeates. The difference in removal performance is due to the dissimilar size and hydrophobicity of each type of DOM. AP is reported to have a low molecular weight (MW) and hydrophobicity [63]; FA [64] and SMP [65] a higher MW compared to AP and neutral hydrophobic and hydrophilic moieties; and HA a high MW and hydrophilic moieties [50]. Therefore, since a significant amount of HA was rejected by the RO membrane and a very low level of SMP was observed in the permeate produced by both MBRs, this has arguably led to a reduction of primary halogenated DBP precursors [66,67], which ultimately would lead to low DBP formation during chlorine or chloramine disinfection for reused water distribution. Since similar fluorescence intensity maps were generated, the AnMBR and AeMBR effluent may have a similar fouling behaviour in terms of DOM, while HA can be hypothesised to have an insignificant role during the RO filtration.

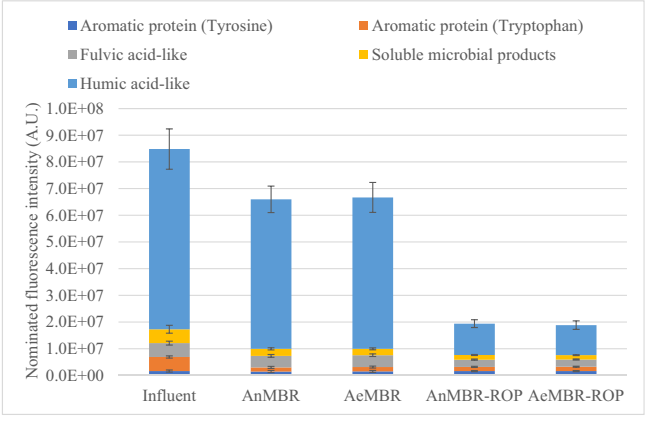

Fig. 3. Distribution of characterized DOM for influent wastewater, AnMBR and AeMBR effluent, AnMBR-ROP and AeMBR-ROP (Better in colour).

3.3. Impact of organic carbon and nitrogen species on RO fouling

Different organics removal performance and different nitrogen species present in the effluent were identified as a distinctive disparity between the performance of the AnMBR and AeMBR. As shown in Fig. 4, the wide distribution of AnMBR effluent TOC concentrations indicate a relatively unstable performance of the biological stage in the AnMBR, while the AeMBR achieved more effective and more robust organic removal, as evidenced by a narrower distribution. Average membrane resistance values of 12.35×10^{13} m^{-1} and 8.97×10^{13} m^{-1} for the AnMBR and AeMBR respectively were recorded, demonstrating a greater fouling propensity of the AnMBR effluent. Noticeably, the average TOC concentration of the AnMBR effluent was 2–3 times higher but the recorded resistance was only about 1.5 time higher compared to AeMBR effluent, suggesting the fouling may not proportionally increase as a function of the TOC concentration. Furthermore, no strong correlation was observed between the membrane resistance and the feed TOC concentration for the AnMBR suggesting that the fouling observed is due to more complex interaction of different compounds. However, the distribution profile partially shows that a higher TOC concentration may lead to higher membrane fouling but in a number instances low fouling was observed for high TOC values suggesting that other factors are also influencing the fouling behaviour. In contrast, there was no such correlation observed for the AeMBR.

A slightly different relationship between the membrane resistance and RO feed characteristics was observed for the AnMBR (Fig. 5.a) and AeMBR (Fig. 5.b) effluents. For the AnMBR effluent, low membrane resistance was observed at low ammonia concentration, and higher resistance was observed with higher ammonia concentration. This could be explained by the different surface charge of ammonia and nitrate in the aquatic environment, where aquatic ammonium presents a single positive charge while nitrate is negative. The membrane used in this study had a negative surface charge, which resulted in electrostatic repulsion of anions [68] and attraction of cations. Therefore ammonium was attracted to maintain a charge balance [69] while simultaneously depositing onto the membrane surface. Furthermore, as more permeate was produced, the pH in the RO cell kept increasing, which led to a constant increase in the ammonia fraction and lowering of the ammonium fraction simultaneously [23]. This ultimately caused a decrease in

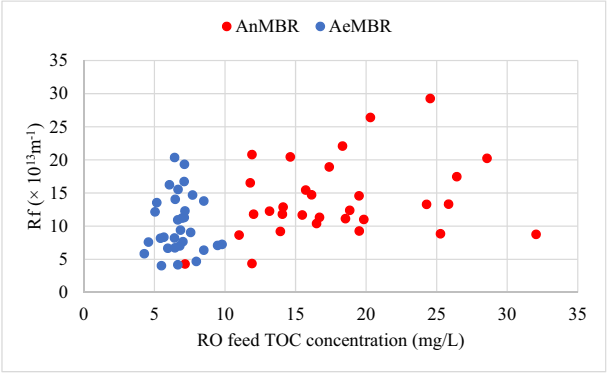

Fig. 4. RO membrane resistance against feed TOC concentration (In colour please). (For interpretation of the references to color in this figure legend, the reader is referred to the online version of this chapter.)

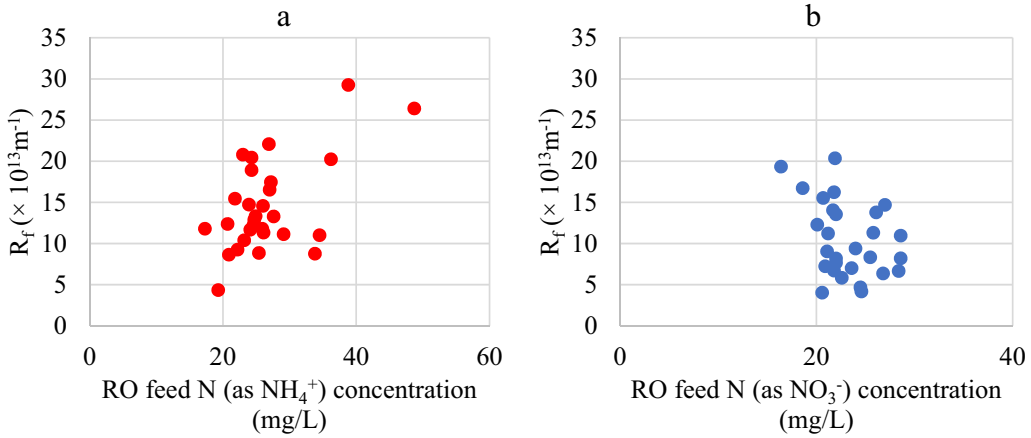

Fig. 5. RO membrane resistance against feed nitrogen concentration (In colour please).

overall ammonia removal performance as uncharged ammonia was more likely to go through the membrane which explains the poorer removal performance. Contrastingly, low membrane resistance was observed at high nitrate concentrations, which can be explained by the nitrate being repulsed by a negative membrane surface charge. Since aquatic nitrate is reported as unreactive [1], this suggested nitrate may not have a significant impact on RO fouling.

Overall, a relatively higher membrane resistance was measured during the filtration of the AnMBR effluent due to a higher total feed organic content when compared to the AeMBR. The presence of ammonium nitrogen in the AnMBR effluent may also contribute to the RO fouling, while the nitrate present in the AeMBR effluent may decrease the fouling. However, no strong correlation was found between membrane resistance and any specific compound.

3.4. RO foulant analysis

3.4.1. Foulant characterization with SEM-EDS

The back scatter electron EDS images for the virgin membrane displayed no bright scatter, which indicated, as expected, that there is no foulant deposited on the membrane surface. After producing 45 mL permeate, the tested membranes of the AnMBR-RO exhibited a large quantity of accumulated bright scatter compared to the AeMBR-RO membranes, indicating more foulant was deposited (Fig. S1 in Supplementary material). Moreover, the random deposit spots observed on the back scatter images for both effluents suggested there was no connection

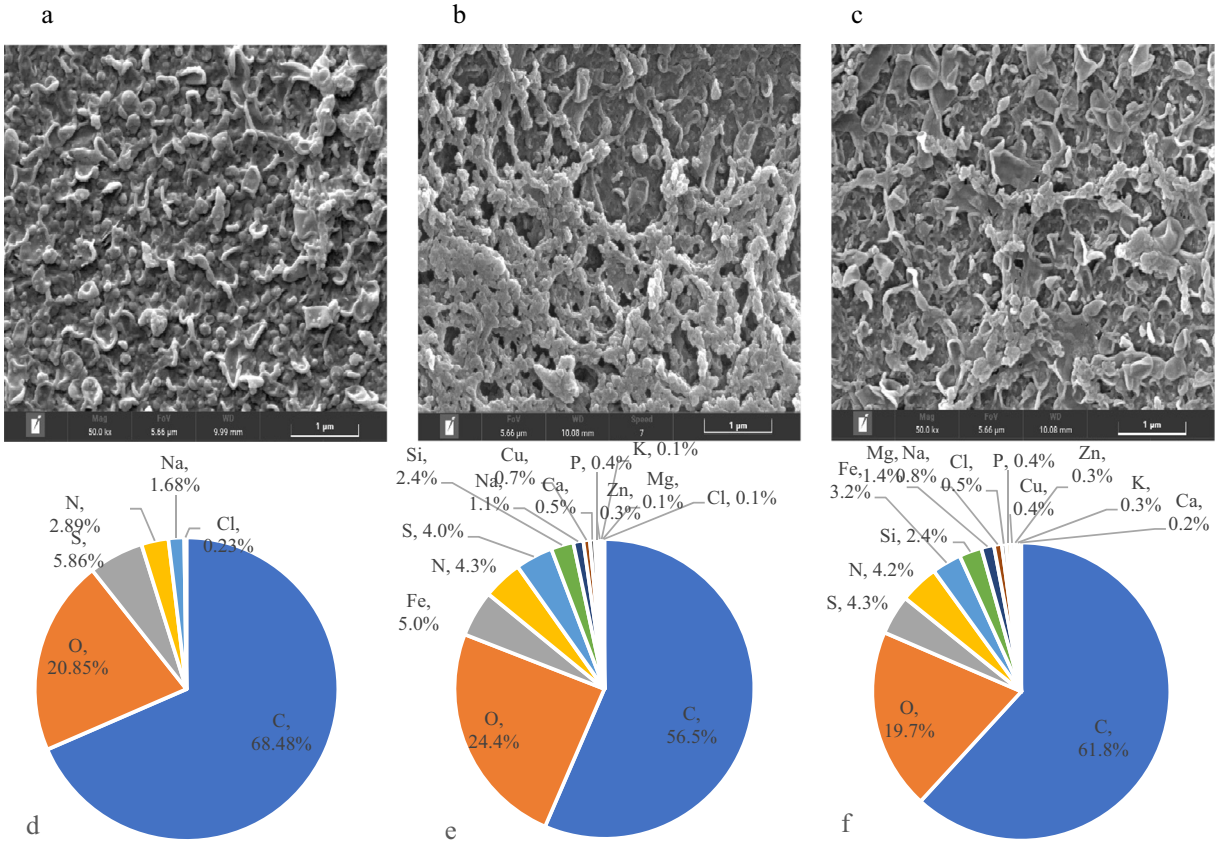

Fig. 6. SEM image and EDS analysis of (a & d) virgin and tested membranes with the (b & e) AnMBR and (c & f) AeMBR (In colour please).

between foulant deposit and membrane surface morphology.

The secondary electron mode in the SEM images generates a gray scale contrast which displays a transitional level of membrane surface topography. A clear cloth type structure could be seen in the virgin membrane image (Fig. 6.a). In contrast, Fig. 6.b and 6.c show comprehensive substance deposition on the used AnMBR-RO and AeMBR-RO membrane surfaces, with the membrane irregularities filled with colloidal material and covered by a multilayer poly-structure. This confirmed the foulant types were organic fouling, inorganic scaling, and colloidal fouling [70–73].

Both images display a colloidal like layer in between and on top of the original membrane structures. The colloidal layer on the AnMBR-RO membranes exhibited complete coverage over the membrane irregularities, while the original membrane surface features were still visible for AeMBR-RO membranes. The multilayer poly-structures observed on the AnMBR-RO membranes had a thicker fouling layer compared to the AeMBR-RO membranes, indicating again a significant level of inorganic substances deposited onto the membrane surface which consequently led to more inorganic fouling. This confirms that the AnMBR effluent contributed to more RO fouling than the AeMBR effluent. This may suggest the priority of foulant deposition during the filtration of MBR effluent is organic and colloidal fouling followed by multilayer scaling of inorganic substances, which confirmed inorganic fouling occurs when the dissolved substances reach their solubility limit in more concentrated solution [70] at higher recovery rates. There was no organism observed in all membrane samples for both MBR effluents, suggesting a low potential of biofouling during the filtration period, which meets the expectation from the results of the coliform tests.

EDS analysis of the virgin membrane (Fig. 6.d) agreed with the reported component characterization of a polyamide-urea-thin film RO membrane, where Carbon and Oxygen account for the most weight percentage [74]. As expected, a variety of deposited substances were detected on both tested membranes, leading to a slight decrease in weight percentage for C, O, S, Na and Cl since more substances were deposited on the membrane surface. However, the weight percentage of N for each membrane increased, indicating deposition of ammonia and nitrate from both the AnMBR and AeMBR effluents. Fe (5 %), N (4.3 %), Si (2.4 %), Cu (0.7 %), Ca (0.5 %), P (0.4 %), Zn (0.3 %), K (0.1 %) and Mg (0.1 %) were identified foulants in the AnMBR effluent. In contrast, foulants deposited from the AeMBR effluent were N (4.2 %), Fe (3.2 %), Si (2.4 %), Mg (1.4 %), P (0.4 %), Cu (0.4 %), Zn (0.3 %), K (0.2 %) and Ca (0.2 %). This agreed with the weight percentage of the foulants on an AeMBR-RO membrane deposit reported by [34,35], with Fe as the highest deposit content by weight. The SEM-EDS analysis also confirms that the AnMBR and AeMBR effluents deposited similar foulants on the RO membranes. However, for the nitrogen species, the small difference observed between the virgin membrane and the fouled membranes should be attributed to ammonia and nitrate for the AnMBR-RO and AeMBR-RO membranes, respectively. However, the co-presence of various foulants may have a further impact on RO fouling [70]. These observations highlight the need to better understand the impact of ammonia and nitrate on RO fouling mechanisms.

3.4.2. Foulant co-presence impact

A multivariate analysis was carried out with the EDS data ($n = 25$) to understand the possible interactions between each deposited substance (Table 3), which may cause more severe fouling compared to the presence of any one foulant on its own [30,45,73]. Although literature sources have commonly reported Ca foulants as calcium sulphate, calcium carbonate, and calcium phosphate [70,75], on the AnMBR-RO membranes, no correlation between Ca and either phosphate or sulphur was observed. Similarly, no association was found between the presence of N and other compounds. However, Ca was found to preferably deposit with N and P for the AeMBR-RO. This may suggest the presence of ammonia and nitrate had a different impact on the scaling of Ca. Likewise, Si has been reported to be deposited in association with phosphate salts [45] which subsequently causes severe fouling with organic matter [30]. Both MBR effluents in this study showed a negative correlation between Si with P and C. However, Si was found to have a significant correlation with O in both effluents, which may suggest silicon dioxide (SiO_2) was formed. Furthermore, Cu was found to not deposit with ammonia on the AnMBR-RO membranes but displayed a high probability to deposit with nitrate on the AeMBR-RO membranes, while phosphate was respectively incongruous to deposit with Fe, Cu and Zn for AnMBR-RO but showed a strong co-deposition correlation on the AeMBR-RO membranes. The positive co-deposition correlation between Mg and O supports previous work which has suggested that the most common Mg foulant is magnesium hydroxide [76]. This meets the expectation that the different behaviour observed were a direct implication of the different effluent matrices from the two systems.

3.4.3. Mass balance of deposited foulants on RO membrane surface (ROS)

In Fig. 7, both columns display a similar structure for foulant mass composition, with Ca as the dominant foulant followed by TOC, nitrogen and phosphate. The rest of the elements only account for 4.56 % and 5.78 % for the AnMBR-ROS and AeMBR-ROS respectively. This agrees with the element types characterized but differ from the mass percentages obtained in the EDS analysis, suggesting the scanned areas may not

Table 3
R values of multivariate correlation matrix of identified foulants for AnMBR-RO (top) and AeMBR-RO (bottom).

AnMBR-RO													
C	-0.13	-0.97	-0.59	-0.26	-0.69	0.03	0.84	0.72	-0.15	-0.19	-0.41	0.17	0.13
-0.32	**N**	-0.05	0.03	-0.21	-0.11	0.48	-0.22	-0.44	-0.10	0.00	-0.10	0.08	0.28
-0.93	0.03	**O**	0.56	0.32	0.73	-0.12	-0.87	-0.66	0.21	0.23	0.39	-0.34	-0.20
0.08	-0.12	-0.24	**Na**	-0.11	0.77	-0.16	-0.44	-0.39	-0.14	-0.11	-0.19	-0.12	-0.11
-0.45	-0.11	0.51	-0.02	**Mg**	0.19	-0.10	-0.34	-0.25	0.67	0.50	0.01	-0.08	-0.10
-0.56	-0.09	0.70	-0.10	0.47	**Si**	-0.24	-0.60	-0.52	0.15	0.02	-0.19	-0.18	-0.15
-0.47	0.13	0.34	-0.07	-0.11	-0.12	**P**	-0.03	-0.34	-0.06	-0.16	0.09	0.03	0.26
0.86	-0.33	-0.75	-0.21	-0.30	-0.51	-0.36	**S**	0.67	-0.39	-0.24	-0.32	0.49	0.15
0.10	-0.13	-0.26	1.00	-0.02	-0.11	-0.08	-0.18	**Cl**	-0.16	-0.33	-0.01	0.05	0.09
-0.09	-0.02	0.14	0.04	-0.04	0.12	-0.13	-0.18	0.02	**K**	0.39	-0.06	-0.10	-0.13
-0.02	0.46	-0.17	0.09	-0.16	-0.14	0.28	-0.14	0.10	-0.06	**Ca**	-0.18	-0.11	-0.03
-0.63	-0.01	0.57	-0.09	0.03	-0.07	0.80	-0.44	-0.11	-0.05	-0.09	**Fe**	-0.10	-0.10
-0.39	0.50	0.17	-0.20	-0.21	-0.22	0.72	-0.32	-0.20	-0.17	0.22	0.59	**Cu**	0.00
-0.46	0.24	0.30	-0.08	-0.12	-0.12	0.96	-0.39	-0.09	-0.10	0.29	0.72	0.82	**Zn**
AeMBR-RO													

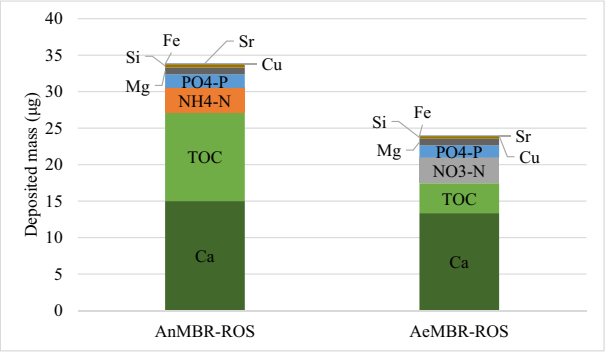

Fig. 7. Deposited foulants mass of AnMBR-ROS and AeMBR-ROS (In colour please).

fully represent the distribution of foulants on the membrane surface.

Deposition on the RO membrane surface was higher for the AnMBR, with a total mass of 33.895 µg compared with 24.010 µg for the AeMBR. TOC (79.9 %) and Ca (16.5 %) were the major components responsible for the difference with no significant difference found for PO_4-P, Mg, Si, Ca, Cu, Fe, and Sr. The difference for TOC can be explained by the initial concentration load onto the RO. However, Ca, along with other substances, constituted a similar load from both MBR effluents, resulting in a slightly higher mass deposited in the AnMBR-ROS compared to the AeMBR-ROS. This may be explained by the fact that the AnMBR-RO had more fouling and that the developed cake layer enhanced the rejection and deposition of other substances [70].

A similar deposition rate excluding ammonia and nitrate was found for both the AnMBR-RO and AeMBR-RO (Table 4). TOC exhibited the highest rate of 67.4 % and 60.7 % for the AnMBR-RO and AeMBR-RO, respectively. This highlights organic fouling is the major fouling mechanism for RO when treating both MBR effluents, a premise supported by the low concentrations of COD and TOC in the RO permeate, as well as a clean fluorescence intensity map. Furthermore, Ca is the major compound for inorganic fouling, where a deposition rate of 30.8 % and 27.1 % was found for AnMBR-RO and AeMBR-RO, respectively. Phosphate and Si respectively exhibited a 5 % deposition rate in both MBR effluents, which are identified as the other major inorganic foulants during the RO filtration. Ammonia exhibited a 13.8 % deposition rate for the AnMBR-RO. This indicates that ammonia is another major inorganic foulant within the AnMBR effluent but contributes less inorganic fouling than Ca. In contrast, nitrate exhibited a much lower deposition rate of 0.02 % for the AeMBR-RO, which confirmed that the presence of nitrate in the AeMBR effluent has a negligible impact on RO fouling. The rest of the foulants demonstrated a much lower deposit rate. This suggested that pre-removal of Ca from the MBR effluents can be a beneficial approach to mitigate RO fouling, since Ca anti-scalants are reported as not effective against the formation and the deposition of calcium based scaling such as calcium phosphate [77,78].

With regard to the circular economy concept, AnMBR-RO can offer a high quality permeate while allowing a potential recovery as fertilizer the rejected nutrients in the RO concentrate, as well as an energy recovery potential to reduce the operational cost [42,71,79–83]. Treating municipal wastewater with a low nutrient concentration may be more suitable for AnMBR-RO in terms of the insufficient ammonia removal in the RO permeate as well as mitigating the RO fouling. Moreover, enhancing the organic removal performance by operating the AnMBR under optimised conditions such as mesophilic temperature, with more precise control, or possibly adding a pre-RO treatment to polish the effluent by removing organics, ammonia and phosphorus could be beneficial to mitigate the RO fouling. However, a more detailed investigation on the trade-offs between the cost of adding an extra barrier to protect the RO or optimising the AnMBR operation and the reduction in energy recovery from the AnMBR when implementing these steps is needed. In contrast, AeMBR-RO has no noticeable limitation when combined with the RO as to the final effluent quality but offers no energy recovery potential. However, adding anaerobic and anoxic zones to the AeMBR can remove the phosphorus and nitrogen while maintaining a high organic removal, hence reducing the RO fouling which could decrease the overall operational expenditure.

4. Conclusions

In this study, a direct performance comparison has been undertaken between the combination of reverse osmosis membranes with AnMBR and AeMBR processes for the treatment of real municipal wastewater for reuse. The analysis focused on a number of previously poorly reported aspects: water quality and trace elements analysis in the context of potable water reuse; the fate of DBP precursors; and characterization of RO membrane foulants - specifically the impact of ammonia and nitrate on RO fouling mechanisms. Major conclusions made were:

1.1. The combination of RO and AeMBR was able to produce a high quality permeate for indirect potable water reuse such as groundwater or drinking water reservoir recharge, while the presence of residual ammonia in the permeate is a current weakness of the AnMBR-RO combination to satisfy the standard threshold. The application of an RO step efficiently removed primary halogenated DBP precursors, resulting in a low DBP formation potential for reused water distribution.

1.2. The AnMBR-RO system experienced more membrane fouling compared to the AeMBR-RO system as evidenced by higher membrane resistance and more deposited substances observed in SEM images. The ammonium nitrogen in the AnMBR effluent may have played a role in RO fouling, while the nitrate in the AeMBR effluent may decrease the fouling due to the effect of surface charge.

1.3. The fouling sequence during the filtration of MBR effluent is organic and colloidal fouling followed then by inorganic scaling. TOC and Ca were identified by weight as the most deposited major foulants in both effluents, and TOC provided a higher deposition rate in both effluents compared to Ca. A higher deposition rate of TOC and Ca was observed during the filtration of the AnMBR effluent in comparison to the AeMBR.

1.4. Ca had a negative correlation with phosphate deposits and none with ammonia where the AnMBR effluent was used but was more likely to deposit with nitrate and phosphate where the AeMBR effluent was used. Ammonia had a 13.8 % deposition ratio during the filtration through the AnMBR-RO, significantly higher than the value of 0.02 % for nitrate when treating the AeMBR effluent.

1.5. Selecting the combination of AnMBR-RO or AeMBR-RO should be based on the influent water matrix as well as the benefit from the recovered energy by AnMBR while also considering additional expenditure for adding treatment steps to protect the RO and control the RO permeate quality.

Table 4
Foulants deposition rate from the AnMBR and AeMBR effluents.

R_D (%)	TOC	Ca	NH_4-N	NO_3-N	PO_4-P	Si	Cu	Sr	Fe	Mg
AnMBR-RO	67.4	30.8	13.8		5.1	5.1	0.08	0.03	0.03	0.02
AeMBR-RO	60.7	27.1		0.02	5.3	5.9	0.06	0.03	0.01	0.02

It is worth mentioning here the relative effectiveness of pre-RO and post-RO disinfection, particularly as pre-RO disinfection has been reported to be an inefficient tool to mitigate RO biofouling [55,84]. Moreover, Al-Abri et al. [85] has reported that pre-RO chlorination may lead to higher overall operational expenditure. The ineffective elimination of generated active chlorine species can cause damage to the membrane polymer, which reduces the lifecycle of RO membranes. However, by controlling the chlorine to ammonia weight dosing ratio [86] during the pre-RO chlorination, the ammonia concentration in AnMBR effluent can be accurately reduced, coupled with a weaker reactivity chloramine being generated compared to chlorine [87] in AeMBR effluent. This highlights a potential mitigation to the unsatisfactory ammonia removal in AnMBR-RO system while producing less DBPs [88] as well as keeping the risk of damage to the membrane surface material to a minimum [89]. On the other hand, the ROP from both MBR effluents in this study exhibited low levels of DBP precursors along with unremoved nutrients and trace elements. Since incomplete removal of trihalomethanes (THMs) and haloacetic acids (HAAs) but no THM or HAA formation for pre-RO and post-RO disinfected MBR effluent has been reported in various studies [31,33,90], this may highlight the need to understand the impact of unremoved substances, specifically the unremoved nitrogen species, on pre-RO or post-RO disinfection processes such as NDMA formation when RO is combined with AnMBR or AeMBR for potable water reuse applications. Moreover, the RO filtration in this study was carried out with a dead-end filtration module with only one type of flat sheet membrane. Future studies carried out with cross flow filtration may provide further insights on fouling behaviour. Furthermore, continuous efforts should be made to understand the impact of foulants (specifically nitrogen species and trace elements) co-presence on RO fouling.

Supplementary data to this article can be found online at https://doi.org/10.1016/j.jwpe.2022.103295.

Declaration of competing interest

The authors declare that they have no known competing financial interests or personal relationships that could have appeared to influence the work reported in this paper.

Data availability

Data will be made available on request.

Acknowledgements

This research did not receive any specific grant from funding agencies in the public, commercial, or not-for-profit sectors.

References

[1] M. Capocelli, V. Piemonte, Technologies for Water Reuse: Current Status and Future Challenges, 2021.
[2] National Research Council, Water Reuse: Potential for Expanding the Nation's Water Supply Through Reuse of Municipal Wastewater, The National Academies Press, Washington, DC, 2012, https://doi.org/10.17226/13303.
[3] T. Asano, F. Burton, H. Leverenz, Water Reuse: Issues, Technologies, and Applications, First edit, McGraw-Hill Education, New York, 2007. https://www.accessengineeringlibrary.com/content/book/9780071459273.
[4] M. Salgot, M. Folch, Wastewater treatment and water reuse, Curr. Opin. Environ. Sci. Heal. 2 (2018) 64–74, https://doi.org/10.1016/j.coesh.2018.03.005.
[5] V. Lazarova, Milestones in Water Reuse: The Best Success Stories, Milestones Water Reuse Best Success Stories, 2015, https://doi.org/10.2166/9781780400716.
[6] H. Lee, T.P. Tan, Singapore's experience with reclaimed water: NEWater, Int. J. Water Resour. Dev. 32 (2016) 611–621, https://doi.org/10.1080/07900627.2015.1120188.
[7] ISO, Water Reuse in Urban Areas. Guidelines for Water Reuse Safety, 2018.
[8] USEPA, Potable reuse compendium. https://www.epa.gov/sites/production/files/2018-01/documents/potablereusecompendium_3.pdf, 2017.
[9] CNEPA, Water Reuse Guildlines GB/T 41016-17-18 2021, 2021.
[10] H.M.K. Delanka-Pedige, S.P. Munasinghe-Arachchige, Y. Zhang, N. Nirmalakhandan, Bacteria and virus reduction in secondary treatment: potential for minimizing post disinfectant demand, Water Res. 177 (2020), 115802, https://doi.org/10.1016/j.watres.2020.115802.
[11] A. Santos, W. Ma, S.J. Judd, Membrane bioreactors: two decades of research and implementation, Desalination 273 (2011) 148–154, https://doi.org/10.1016/j.desal.2010.07.063.
[12] C. Shin, J. Bae, Current status of the pilot-scale anaerobic membrane bioreactor treatments of domestic wastewaters: a critical review, Bioresour. Technol. 247 (2018) 1038–1046, https://doi.org/10.1016/j.biortech.2017.09.002.
[13] K.M. Wang, D. Cingolani, A.L. Eusebi, A. Soares, B. Jefferson, E.J. McAdam, Identification of gas sparging regimes for granular anaerobic membrane bioreactor to enable energy neutral municipal wastewater treatment, J. Membr. Sci. 555 (2018) 125–133, https://doi.org/10.1016/j.memsci.2018.03.032.
[14] T. Wintgens, T. Melin, A. Schäfer, S. Khan, M. Muston, D. Bixio, C. Thoeye, The role of membrane processes in municipal wastewater reclamation and reuse, Desalination 178 (2005) 1–11, https://doi.org/10.1016/j.desal.2004.12.014.
[15] A. Plevri, D. Mamais, C. Noutsopoulos, C. Makropoulos, A. Andreadakis, K. Rippis, E. Smeti, E. Lytras, C. Lioumis, Promoting on-site urban wastewater reuse through MBR-RO treatment, Desalin. Water Treat. 91 (2017) 2–11, https://doi.org/10.5004/dwt.2017.20804.
[16] P. Jeffrey, Z. Yang, S.J. Judd, The status of potable water reuse implementation, Water Res. 214 (2022), 118198, https://doi.org/10.1016/j.watres.2022.118198.
[17] M. Shen, S. Keten, R.M. Lueptow, Rejection mechanisms for contaminants in polyamide reverse osmosis membranes, J. Membr. Sci. 509 (2016) 36–47, https://doi.org/10.1016/j.memsci.2016.02.043.
[18] Z. Shareefdeen, A. Elkamel, S. Kandhro, Modern water reuse technologies: membrane bioreactors, in: S. Eslamian (Ed.), Urban Water Reuse Handb, 1st ed., CRC Press, Boca Raton, 2015, pp. 383–392, https://doi.org/10.1201/b19646-41.
[19] A. Plevri, C. Noutsopoulos, D. Mamais, C. Makropoulos, A. Andreadakis, E. Lytras, S. Samios, Priority pollutants and other micropollutants removal in an mbr-ro wastewater treatment system, Desalin. Water Treat. 127 (2018) 121–131, https://doi.org/10.5004/dwt.2018.22857.
[20] Y. Zhai, G. Liu, W.G.J. van der Meer, One-step reverse osmosis based on riverbank filtration for future drinking water purification, Engineering (2021), https://doi.org/10.1016/j.eng.2021.02.015.
[21] PUB, PUB NEWater quality. https://www.pub.gov.sg/watersupply/waterquality/newater, 2019.
[22] J. Gu, H. Liu, S. Wang, M. Zhang, Y. Liu, An innovative anaerobic MBR-reverse osmosis-ion exchange process for energy-efficient reclamation of municipal wastewater to NEWater-like product water, J. Clean. Prod. 230 (2019) 1287–1293, https://doi.org/10.1016/j.jclepro.2019.05.198.
[23] C. Shin, A. Szczuka, R. Jiang, W.A. Mitch, C.S. Criddle, Optimization of reverse osmosis operational conditions to maximize ammonia removal from the effluent of an anaerobic membrane bioreactor, Environ. Sci. Water Res. Technol. 7 (2021) 739–747, https://doi.org/10.1039/d0ew01112f.
[24] H. Liu, J. Gu, S. Wang, M. Zhang, Y. Liu, Performance, membrane fouling control and cost analysis of an integrated anaerobic fixed-film MBR and reverse osmosis process for municipal wastewater reclamation to NEWater-like product water, J. Membr. Sci. 593 (2020), 117442, https://doi.org/10.1016/j.memsci.2019.117442.
[25] N. Zaouri, H. Cheng, F. Khairunnisa, A. Alahmed, I. Blilou, P.Y. Hong, A type dependent effect of treated wastewater matrix on seed germination and food production, Sci. Total Environ. 769 (2021), 144573, https://doi.org/10.1016/j.scitotenv.2020.144573.
[26] W. Liu, X. Song, N. Huda, M. Xie, G. Li, W. Luo, Comparison between aerobic and anaerobic membrane bioreactors for trace organic contaminant removal in wastewater treatment, Environ. Technol. Innov. 17 (2020), 100564, https://doi.org/10.1016/j.eti.2019.100564.
[27] S.D. Kim, J. Cho, I.S. Kim, B.J. Vanderford, S.A. Snyder, Occurrence and removal of pharmaceuticals and endocrine disruptors in south korean surface, drinking, and waste waters, Water Res. 41 (2007) 1013–1021, https://doi.org/10.1016/j.watres.2006.06.034.
[28] J. Mamo, M.J. García-Galán, M. Stefani, S. Rodríguez-Mozaz, D. Barceló, H. Monclús, I. Rodriguez-Roda, J. Comas, Fate of pharmaceuticals and their transformation products in integrated membrane systems for wastewater reclamation, Chem. Eng. J. 331 (2018) 450–461, https://doi.org/10.1016/j.cej.2017.08.050.
[29] A.A. Alturki, N. Tadkaew, J.A. McDonald, S.J. Khan, W.E. Price, L.D. Nghiem, Combining MBR and NF/RO membrane filtration for the removal of trace organics in indirect potable water reuse applications, J. Membr. Sci. 365 (2010) 206–215, https://doi.org/10.1016/j.memsci.2010.09.008.
[30] K. Kimura, S. Okazaki, T. Ohashi, Y. Watanabe, Importance of the co-presence of silica and organic matter in membrane fouling for RO filtering MBR effluent, J. Membr. Sci. 501 (2016) 60–67, https://doi.org/10.1016/j.memsci.2015.12.016.
[31] A.M. Comerton, R.C. Andrews, D.M. Bagley, Evaluation of an MBR–RO system to produce high quality reuse water: microbial control, DBP formation and nitrate, Water Res. 39 (2005) 3982–3990, https://doi.org/10.1016/j.watres.2005.07.014.
[32] A.M. Comerton, R.C. Andrews, D.M. Bagley, Impact of blending reuse and lake water on treated water quality, J. Environ. Eng. Sci. 5 (2006) 359–363, https://doi.org/10.1139/s05-042.
[33] M.A. Zazouli, L.R. Kalankesh, Removal of precursors and disinfection byproducts (DBPs) by membrane filtration from water; a review, J. Environ. Health Sci. Eng. 15 (2017) 25, https://doi.org/10.1186/s40201-017-0285-z.
[34] F. Tang, H.Y. Hu, L.J. Sun, Q.Y. Wu, Y.M. Jiang, Y.T. Guan, J.J. Huang, Fouling of reverse osmosis membrane for municipal wastewater reclamation: autopsy results from a full-scale plant, Desalination 349 (2014) 73–79, https://doi.org/10.1016/j.desal.2014.06.018.

[35] F. Tang, H.Y. Hu, L.J. Sun, Y.X. Sun, N. Shi, J.C. Crittenden, Fouling characteristics of reverse osmosis membranes at different positions of a full-scale plant for municipal wastewater reclamation, Water Res. 90 (2016) 329–336, https://doi.org/10.1016/j.watres.2015.12.028.
[36] Apha, Standard methods for the examination of water and wastewater standard methods for the examination of water and wastewater, Public Health 51 (1999), https://doi.org/10.2105/AJPH.51.6.940-a, 940-940.
[37] W. Chen, P. Westerhoff, J.A. Leenheer, K. Booksh, Fluorescence excitation-emission matrix regional integration to quantify spectra for dissolved organic matter, Environ. Sci. Technol. 37 (2003) 5701–5710, https://doi.org/10.1021/es034354c.
[38] S. Pan, X. Chen, C. Cao, Z. Chen, H. Hao Ngo, Q. Shi, W. Guo, H.Y. Hu, Fluorescence analysis of centralized water supply systems: indications for rapid cross-connection detection and water quality safety guarantee, Chemosphere 277 (2021), 130290, https://doi.org/10.1016/j.chemosphere.2021.130290.
[39] D.J. Lapworth, D.G. Kinniburgh, An R script for visualising and analysing fluorescence excitation-emission matrices (EEMs), Comput. Geosci. 35 (2009) 2160–2163, https://doi.org/10.1016/j.cageo.2008.10.013.
[40] C. Visvanathan, A. Abeynayaka, Developments and future potentials of anaerobic membrane bioreactors (AnMBRs), Membr. Water Treat. 3 (2012) 1–23, https://doi.org/10.12989/mwt.2012.3.1.001.
[41] C.Y. Tang, Z. Yang, H. Guo, J.J. Wen, L.D. Nghiem, E. Cornelissen, Potable water reuse through advanced membrane technology, Environ. Sci. Technol. 52 (2018) 10215–10223, https://doi.org/10.1021/acs.est.8b00562.
[42] X. Song, W. Luo, F.I. Hai, W.E. Price, W. Guo, H.H. Ngo, L.D. Nghiem, Resource recovery from wastewater by anaerobic membrane bioreactors: opportunities and challenges, Bioresour. Technol. 270 (2018) 669–677, https://doi.org/10.1016/j.biortech.2018.09.001.
[43] A. Foglia, G. Cipolletta, N. Frison, S. Sabbatini, S. Gorbi, A.L. Eusebi, F. Fatone, Anaerobic membrane bioreactor for urban wastewater valorisation: operative strategies and fertigation reuse, Chem. Eng. Trans. 74 (2019) 247–252, https://doi.org/10.3303/CET1974042.
[44] C. Martínez, V. Gómez, E. Pocurull, F. Borrull, Characterization of organic fouling in reverse osmosis membranes by headspace solid phase microextraction and gas chromatography-mass spectrometry, Water Sci. Technol. 71 (2015) 117–125, https://doi.org/10.2166/wst.2014.475.
[45] M. Malki, V. Abbas, Relationship between phosphate scales and silica fouling in wastewater RO membrane systems, IDA J. Desalin. Water Reuse 5 (2013) 15–24, https://doi.org/10.1179/2051645213y.0000000003.
[46] M.H. Gerardi, Nitrifying bacteria, in: Nitrification Denitrification Act. Sludge Process, John Wiley & Sons, Ltd, 2002, pp. 43–54, https://doi.org/10.1002/0471216682.ch7.
[47] J. Arévalo, L.M. Ruiz, J. Pérez, B. Moreno, M.Á. Gómez, Removal performance of heavy metals in MBR systems and their influence in water reuse, Water Sci. Technol. J. Int. Assoc. Water Pollut. Res. 67 (2013) 894–900, https://doi.org/10.2166/wst.2012.620.
[48] PUB, PUB NEWater quality standards. https://www.pub.gov.sg/watersupply/fournationaltaps/newater, 2020.
[49] J.-J. Qin, M.H. Oo, B. Coniglio, Relationship between feed pH and permeate pH in reverse osmosis with town water as feed, Desalination 177 (2005) 267–272, https://doi.org/10.1016/j.desal.2004.11.022.
[50] D. Ma, Y. Meng, C. Xia, B. Gao, Y. Wang, Fractionation, characterization and C-, N-disinfection byproduct formation of soluble microbial products in MBR processes, Bioresour. Technol. 198 (2015) 380–387, https://doi.org/10.1016/j.biortech.2015.09.043.
[51] M.A. Al-Obaidi, J.-P. Li, S. Alsadaie, C. Kara-Zaïtri, I.M. Mujtaba, Modelling and optimisation of a multistage reverse osmosis processes with permeate reprocessing and recycling for the removal of N-nitrosodimethylamine from wastewater using species conserving genetic algorithms, Chem. Eng. J. 350 (2018) 824–834, https://doi.org/10.1016/j.cej.2018.06.022.
[52] T. Fujioka, K.P. Ishida, T. Shintani, H. Kodamatani, High rejection reverse osmosis membrane for removal of N-nitrosamines and their precursors, Water Res. 131 (2018) 45–51, https://doi.org/10.1016/j.watres.2017.12.025.
[53] L. Masse, M. Mondor, J. Dubreuil, Effect of pH level and acid type on total ammoniacal nitrogen (TAN) retention and fouling of reverse osmosis membranes processing swine wastewater, Water Qual. Res. J. Can. 50 (2015) 297–304, https://doi.org/10.2166/wqrjc.2015.143.
[54] B. Cancino-Madariaga, C.F. Hurtado, R. Ruby, Effect of pressure and pH in ammonium retention for nanofiltration and reverse osmosis membranes to be used in recirculation aquaculture systems (RAS), Aquac. Eng. 45 (2011) 103–108, https://doi.org/10.1016/j.aquaeng.2011.08.002.
[55] S. Gare, RO systems: the importance of pre-treatment, Filtr. Sep. - FILTR SEP. 39 (2002) 22–27, https://doi.org/10.1016/S0015-1882(02)80047-7.
[56] H. Huang, B.-Y. Chen, Z.-R. Zhu, Formation and speciation of haloacetamides and haloacetonitriles for chlorination, chloramination, and chlorination followed by chloramination, Chemosphere 166 (2017) 126–134, https://doi.org/10.1016/j.chemosphere.2016.09.047.
[57] A. Kapoor, T. Viraraghavan, Nitrate removal from drinking water—review, J. Environ. Eng. 123 (1997) 371–380, https://doi.org/10.1061/(asce)0733-9372(1997)123:4(371).
[58] K.L. Tu, L.D. Nghiem, A.R. Chivas, Boron removal by reverse osmosis membranes in seawater desalination applications, Sep. Purif. Technol. 75 (2010) 87–101, https://doi.org/10.1016/j.seppur.2010.07.021.
[59] N. Chaukura, S.S. Marais, W. Moyo, N. Mbali, L.C. Thakalekoala, T. Ingwani, B. B. Mamba, P. Jarvis, T.T.I. Nkambule, Contemporary issues on the occurrence and removal of disinfection byproducts in drinking water - a review, J. Environ. Chem. Eng. 8 (2020), 103659, https://doi.org/10.1016/j.jece.2020.103659.
[60] C.Y. Tang, Y.-N. Kwon, J.O. Leckie, Characterization of humic acid fouled reverse osmosis and nanofiltration membranes by transmission electron microscopy and streaming potential measurements, Environ. Sci. Technol. 41 (2007) 942–949, https://doi.org/10.1021/es061322r.
[61] C.Y. Tang, Y.-N. Kwon, J.O. Leckie, Fouling of reverse osmosis and nanofiltration membranes by humic acid—effects of solution composition and hydrodynamic conditions, J. Membr. Sci. 290 (2007) 86–94, https://doi.org/10.1016/j.memsci.2006.12.017.
[62] J. Liu, M. Zhao, C. Duan, P. Yue, T. Li, Removal characteristics of dissolved organic matter and membrane fouling in ultrafiltration and reverse osmosis membrane combined processes treating the secondary effluent of wastewater treatment plant, Water Sci. Technol. 83 (2020) 689–700, https://doi.org/10.2166/wst.2020.589.
[63] G.D. Rose, in: W.J. Lennarz, M.D.B.T.-E. of B.C. Lane (Eds.), Secondary Structure in Protein Analysis, Elsevier, New York, 2004, pp. 1–6, https://doi.org/10.1016/B0-12-443710-9/00613-X.
[64] S. Hiradate, T. Yonezawa, H. Takesako, Isolation and purification of hydrophilic fulvic acids by precipitation, Geoderma 132 (2006) 196–205, https://doi.org/10.1016/j.geoderma.2005.05.007.
[65] D.C. Banti, P. Samaras, C. Tsioptsias, A. Zouboulis, M. Mitrakas, Mechanism of SMP aggregation within the pores of hydrophilic and hydrophobic MBR membranes and aggregates detachment, Sep. Purif. Technol. 202 (2018) 119–129, https://doi.org/10.1016/j.seppur.2018.03.045.
[66] D. Ma, C. Xia, B. Gao, Q. Yue, Y. Wang, C-, N-DBP formation and quantification by differential spectra in MBR treated municipal wastewater exposed to chlorine and chloramine, Chem. Eng. J. 291 (2016) 55–63, https://doi.org/10.1016/j.cej.2016.01.091.
[67] T. Bond, E.H. Goslan, S.A. Parsons, B. Jefferson, Treatment of disinfection by-product precursors, Environ. Technol. 32 (2011) 1–25, https://doi.org/10.1080/09593330.2010.495138.
[68] M.A. Alghoul, P. Poovanaesvaran, K. Sopian, M.Y. Sulaiman, Review of brackish water reverse osmosis (BWRO) system designs, Renew. Sust. Energ. Rev. 13 (2009) 2661–2667, https://doi.org/10.1016/j.rser.2009.03.013.
[69] T. Hoang, G. Stevens, S. Kentish, The effect of feed pH on the performance of a reverse osmosis membrane, Desalination 261 (2010) 99–103, https://doi.org/10.1016/j.desal.2010.05.024.
[70] S. Jiang, Y. Li, B.P. Ladewig, A review of reverse osmosis membrane fouling and control strategies, Sci. Total Environ. 595 (2017) 567–583, https://doi.org/10.1016/j.scitotenv.2017.03.235.
[71] M. Xie, H.K. Shon, S.R. Gray, M. Elimelech, Membrane-based processes for wastewater nutrient recovery: technology, challenges, and future direction, Water Res. 89 (2016) 210–221, https://doi.org/10.1016/j.watres.2015.11.045.
[72] Z. Hu, A. Antony, G. Leslie, P. Le-Clech, Real-time monitoring of scale formation in reverse osmosis using electrical impedance spectroscopy, J. Membr. Sci. 453 (2014) 320–327, https://doi.org/10.1016/j.memsci.2013.11.014.
[73] H.Z. Shafi, A. Matin, S. Akhtar, K.K. Gleason, S.M. Zubair, Z. Khan, Organic fouling in surface modified reverse osmosis membranes: filtration studies and subsequent morphological and compositional characterization, J. Membr. Sci. 527 (2017) 152–163, https://doi.org/10.1016/j.memsci.2017.01.017.
[74] L.F. Liu, S.C. Yu, Y. Zhou, C.J. Gao, Study on a novel polyamide-urea reverse osmosis composite membrane (ICIC-MPD). I. Preparation and characterization of ICIC-MPD membrane, J. Membr. Sci. 281 (2006) 88–94, https://doi.org/10.1016/j.memsci.2006.03.012.
[75] J.M. Ochando-Pulido, M.D. Victor-Ortega, A. Martínez-Ferez, On the cleaning procedure of a hydrophilic reverse osmosis membrane fouled by secondary-treated olive mill wastewater, Chem. Eng. J. 260 (2015) 142–151, https://doi.org/10.1016/j.cej.2014.08.094.
[76] S. Patel, J. Milligan, Magnesium hydroxide deposit control for reverse osmosis systems, in: NACE - Int. Corros. Conf. Ser, 2008, 083741–0837414.
[77] M.N. Mangal, S.G. Salinas-Rodriguez, J. Dusseldorp, A.J.B. Kemperman, J. C. Schippers, M.D. Kennedy, W.G.J. van der Meer, Effectiveness of antiscalants in preventing calcium phosphate scaling in reverse osmosis applications, J. Membr. Sci. 623 (2021), 119090, https://doi.org/10.1016/j.memsci.2021.119090.
[78] M.N. Mangal, S.G. Salinas-Rodriguez, J. Dusseldorp, B. Blankert, V.A. Yangali-Quintanilla, A.J.B. Kemperman, J.C. Schippers, W.G.J. van der Meer, M. D. Kennedy, Foulant identification and performance evaluation of antiscalants in increasing the recovery of a reverse osmosis system treating anaerobic groundwater, Membranes (Basel) 12 (2022) 290, https://doi.org/10.3390/membranes12030290.
[79] P.L. McCarty, J. Bae, J. Kim, Domestic wastewater treatment as a net energy producer-can this be achieved? Environ. Sci. Technol. 45 (2011) 7100–7106, https://doi.org/10.1021/es2014264.
[80] V. Stazi, M.C. Tomei, Enhancing anaerobic treatment of domestic wastewater: state of the art, innovative technologies and future perspectives, Sci. Total Environ. (2018), https://doi.org/10.1016/j.scitotenv.2018.04.071.
[81] A. Sendrowski, T.H. Boyer, Phosphate removal from urine using hybrid anion exchange resin, Desalination 322 (2013) 104–112, https://doi.org/10.1016/j.desal.2013.05.014.
[82] S.P. Mallick, D.R. Ryan, K. Venkiteshwaran, P.J. McNamara, B.K. Mayer, Electro-oxidation to convert dissolved organic nitrogen and soluble non-reactive phosphorus to more readily removable and recoverable forms, Chemosphere 279 (2021), 130876, https://doi.org/10.1016/j.chemosphere.2021.130876.
[83] X. Huang, S. Guida, B. Jefferson, A. Soares, Economic evaluation of ion-exchange processes for nutrient removal and recovery from municipal wastewater, Npj Clean Water 3 (2020), https://doi.org/10.1038/s41545-020-0054-x.

[84] S.F. Anis, R. Hashaikeh, N. Hilal, Reverse osmosis pretreatment technologies and future trends: a comprehensive review, Desalination 452 (2019) 159–195, https://doi.org/10.1016/j.desal.2018.11.006.
[85] M. Al-Abri, B. Al-Ghafri, T. Bora, S. Dobretsov, J. Dutta, S. Castelletto, L. Rosa, A. Boretti, Chlorination disadvantages and alternative routes for biofouling control in reverse osmosis desalination, Npj Clean Water 2 (2019) 2, https://doi.org/10.1038/s41545-018-0024-8.
[86] D.G. Wahman, Web-based applications to simulate drinking water inorganic chloramine chemistry, J. Am. Water Works Assoc. 110 (2018) E43–E61, https://doi.org/10.1002/awwa.1146.
[87] G. Hua, D.A. Reckhow, I. Abusallout, Correlation between SUVA and DBP formation during chlorination and chloramination of NOM fractions from different sources, Chemosphere 130 (2015) 82–89, https://doi.org/10.1016/j.chemosphere.2015.03.039.
[88] M.J. Farré, K. Doederer, W. Gernjak, Y. Poussade, H. Weinberg, Disinfection by-products management in high quality recycled water, Water Sci. Technol. Water Supply 12 (2012) 573–579, https://doi.org/10.2166/ws.2012.031.
[89] M.J. Cran, S.W. Bigger, S.R. Gray, Degradation of polyamide reverse osmosis membranes in the presence of chloramine, Desalination 283 (2011) 58–63, https://doi.org/10.1016/j.desal.2011.04.050.
[90] K. Kimura, G. Amy, J.E. Drewes, T. Heberer, T.-U. Kim, Y. Watanabe, Rejection of organic micropollutants (disinfection by-products, endocrine disrupting compounds, and pharmaceutically active compounds) by NF/RO membranes, J. Membr. Sci. 227 (2003) 113–121, https://doi.org/10.1016/j.memsci.2003.09.005.